Molecular and Cellular Biochemistry (2020) 475:215–226
https://doi.org/10.1007/s11010-020-03874-9

Crosstalk between Noxa, Bcl-2, and ceramide in mediating p53-dependent apoptosis in Molt-4 human T-cell leukemia

Hadile Kobeissy[1] · Rouba Hage-Sleiman[2] · Zeinab Dakdouk[1] · Lina Kozhaya[1] · Ghassan Dbaibo[1,3]

Received: 21 April 2020 / Accepted: 1 August 2020 / Published online: 7 August 2020

Abstract

Ionizing radiation induces apoptosis in human Molt-4 leukemia cells in a p53-dependent manner. The tumor suppressor p53 stimulates various downstream targets that presumably trigger, individually or in concert, de novo ceramide synthesis and intrinsic apoptosis via mitochondrial outer membrane permeabilization (MOMP). Among these targets, BH3-only protein Noxa was found to be promptly activated by p53 prior to ceramide accumulation and apoptosis in response to irradiation. To evaluate the relation between Noxa and ceramide in irradiation-induced apoptosis, *Noxa* was silenced in Molt-4 cells and apoptosis, p53 expression, and ceramide accumulation were assessed in response to irradiation. In the absence of *Noxa*, irradiation of Molt-4 cells still induced apoptosis in a p53-dependent manner however ceramide levels decreased significantly although they remained higher than untreated control. Upon irradiation, Noxa was found to translocate to the mitochondria where endogenous ceramide accumulation was observed. In contrast, overexpression of Bcl-2, another mitochondrial protein, in Molt-4 cells abolished the endogenous ceramide accumulation and apoptosis. In irradiation-induced, p53-dependent pathways of apoptosis, the pro-apoptotic Noxa represents one of several, yet to be identified, pathways simultaneously triggered by p53 to produce mitochondrial ceramide accumulation and apoptosis. In contrast, Bcl-2 functions as a broader inhibitor of both ceramide accumulation and apoptosis. Altogether, these results indicate that members of the Bcl-2 family differentially regulate ceramide accumulation and reveal the existence of crosstalk between Bcl-2 family members and ceramide in mediating p53-dependent apoptosis in Molt-4 human T-cell leukemia.

Keywords p53 · Noxa · Ceramide · Bcl-2 · Mitochondrial apoptosis · Cancer

Introduction

Apoptosis is an orchestrated self-destruction mechanism induced by a variety of stressors such as hypoxia/hyperoxia, irradiation, ultra-violet (UV) light, tumor necrosis factor α (TNF), and TNF-related apoptosis-inducing ligand (TRAIL) [1]. In most of the cases, these stimuli trigger caspase activation [2]. Based on the type of activated caspases, apoptosis is classified into two major pathways extrinsic and intrinsic. Extrinsic apoptosis or death receptor-mediated pathway propagates a signaling cascade that is initiated by the binding of death ligands such as FasL and TRAIL to their corresponding receptors followed by cleavage of caspase 8 and generation of truncated Bid (tBid), a Bcl-2 family member. However, the intrinsic mitochondrial pathway is mainly triggered by non-receptor stimuli that induce the expression of p53, which in its turn regulates, apart from Bid, different Bcl-2 family members that consequently activate caspase 9 [3, 4]. Finally, both forms of apoptosis merge into one execution pathway involving activation of terminal caspase 3 and DNA fragmentation.

A key event in extrinsic and intrinsic apoptosis is the mitochondrial disruption regulated by Bcl-2 family proteins [5]. The Bcl-2 family members include the anti- and pro- apoptotic proteins. Deviation in the dynamic balance

✉ Rouba Hage-Sleiman
rouba.hagesleiman@ul.edu.lb

✉ Ghassan Dbaibo
gdbaibo@aub.edu.lb

[1] Department of Biochemistry and Molecular Genetics, Faculty of Medicine, American University of Beirut, Beirut, Lebanon

[2] Department of Biology, Faculty of Sciences, Lebanese University, Hadath, Lebanon

[3] Department of Pediatrics and Adolescent Medicine, Center for Infectious Diseases Research, Faculty of Medicine, American University of Beirut, Beirut, Lebanon

between these two groups results in either inhibition or promotion of apoptosis. It was shown that p53, once activated, could transcriptionally activate pro-apoptotic Bcl-2 Homology domain-3 (BH3)-only genes such as p53 upregulated modulator of apoptosis (PUMA) and phorbol-12-myristate-13-acetate-induced protein 1 (PMAIP1 or Noxa) [6]. These BH3-only pro-apoptotic proteins, as their name indicates, possess only one of the sequence-homolog domains in contrast to other members that have four domains (BH1-4). These proteins, in addition to tBid, induce apoptosis by directly or indirectly activating the Bcl-2 family executioners Bax and/or Bak, which in turn oligomerize and induce mitochondrial outer membrane permeabilization (MOMP) [7–10]. MOMP is a process of mitochondrial pore formation leading to loss of mitochondrial transmembrane potential followed by a release of mitochondrial apoptogenic proteins from the transmembrane space into the cytosol [1]. These proteins are cytochrome c, SMAC/DIABLO, and apoptosis-inducing factor (AIF). Released cytochrome c will eventually cause caspase 3 cleavage, PARP cleavage, and subsequent apoptosis.

Likewise, ceramide, a signaling sphingolipid, induces apoptosis through MOMP initiation [11]. Ceramide enzymes found on the mitochondrial inner and outer membranes include ceramidase and ceramide synthase [12]. Similarly, sphingomyelinase, sphingomyelin synthase, and ceramide synthase located in close proximity to the mitochondria can also synthesize ceramides that can translocate to the mitochondria upon stress via ceramide transfer proteins (CERT), vesicles, or mitochondrial-associated membranes (MAMs) [2]. The synthesized ceramides then form channels and fuse with the mitochondrial membrane resulting in the decrease of inner mitochondrial potential and initiation of MOMP. Interestingly, the formation of Bax oligomers and ceramide channels work synergistically in initiating MOMP where the resulting permeability exceeds that of either Bax or ceramide added alone [13].

We have previously shown that ceramide accumulates in a p53-dependent manner in response to γ-irradiation of Molt-4 leukemia cells [4]. We also demonstrated that this ceramide accumulation is mostly synthesized de novo to yield predominantly N-palmitoylsphingosine (C16-ceramide) [14]. Additionally, we explored the potential p53-regulated genes that are differentially expressed in response to irradiation of Molt-4 cells at two time points, 3 and 8 h, before any ceramide accumulation occurs in order to identify candidate genes that mediate the p53 regulation of ceramide synthesis [15]. Among many candidate genes identified, PMAIP1/Noxa (FC = 2.27) was upregulated after 3 h of irradiation in Molt-4 cells [15]. Thus, we hypothesized that Noxa may be a possible mediator of the effects of p53 on ceramide and subsequent apoptosis.

Materials and methods

Cellular models and cell culture

Human T cell leukemia Molt-4 cells were obtained from American Type Culture Collection (ATCC). Molt-4-LXSN cells (stably transfected with empty retroviral vector LXSN) and Molt-4-E6 (stably transfected with the human papillomavirus E6 gene cloned into the LXSN retroviral vector, a kind gift from Dr. Denise Galloway, University of Washington, Seattle, WA) were cultured in RPMI 1640 supplemented with 10% fetal bovine serum (Sigma; F9665) and 1% penicillin–streptomycin, and maintained by selection with 0.5 mg/ml geneticin (G418) at 37 °C in a humidified atmosphere containing 5% CO_2. Molt-4 cells were irradiated with 5 Gy of γ rays using a Cesium source 137Cs (2441.1 cGy/min).

Establishment of stable transfectants

Transfections of Molt-4 cells were performed using Amaxa cell line nucleofector kit L (Lonza technique) according to the manufacturer's recommendation. Stable transfectants were established by transfecting Molt-4 cells with shRNA scrambled (*ggaatctcattcgatgcatac*) and shRNA *Noxa* (*tccatatatgcattggtgaat*) (Qiagen) to obtain Molt-4-SCR and Molt-4-KD^{NOXA} cells, respectively. Molt-4 cells stably transfected with MEP4 empty vector and MEP4 vector expressing Bcl-2 were designated Molt-4 MEP4 and Molt-4 Bcl-2, respectively. Cells were cultured in RPMI 1640 supplemented with 10% fetal bovine serum and 1% penicillin–streptomycin, and maintained by selection with 0.5 mg/ml hygromycin at 37 °C in a humidified atmosphere containing 5% CO_2.

Cell death assay

Cell death was studied using the trypan Blue exclusion assay. Molt-4 cells were seeded at a density of 5×10^6 cells in T25 flasks and irradiated with 5 Gy of γ rays for 6, 10, and 24 h. At each time point, cells were harvested, pelleted, and stained with trypan blue (ratio 1:1). Cells were then counted using a hemocytometer. The counts of dead cells (darkly stained) and alive cells (clear) were then computed.

Annexin V/PI assay

At each time point, cells were collected by centrifugation at 2000 rpm for 10 min. Then using Annexin-V-FLUOS Staining Kit from Roche, pellets were incubated with 100 µl of incubation buffer, 2 µl of Annexin-V-FITC labeling agent and 2 µl propidium iodide solution, and then kept for 15 min

at room temperature in the dark. Cells were read by flow cytometry (Guava easyCyte, Millipore) and 10,000 events were counted and results were analyzed using the Incyte software. Alive cells are negatively stained for both Annexin V and PI. Early apoptotic cells are Annexin V positive and PI negative. Late apoptotic cells are both Annexin V and PI positive. Necrotic cells are Annexin V negative and PI positive.

Lipid extraction and phosphate assay

Cells at a density of 10×10^6 per condition were pelleted at different time points in borosilicate glass tubes, washed with PBS, suspended in a ratio of 2:1 methanol to chloroform and stored at − 80 °C for 2–3 days [16]. Then the aqueous and lipid phases were separated using a mixture of methanol/chloroform/water ratio 2:2:1.7 and centrifuged at 2500 rpm for 10 min. The resulting lipid phase (lower phase) of each sample was then transferred into a new glass tube to be dried by speed vacuum. Finally, the invisible pellet was suspended in 1 ml chloroform, and 200 µl was aliquoted to determine the phosphate concentration in the samples. Lipid phosphates were measured as in the method of Rouser et al. [17]. After thawing at room temperature, the samples were dried by speed vacuum and then 150 µl of perchloric acid (70%) was added. The reaction was allowed to proceed for 1 h at 180 °C. Then, the samples were cooled and 830 µl of water was added, followed by 170 µl of ammonium molybdate (2.5%) and 170 µl of freshly prepared ascorbic acid (10%). The mixture was incubated in a water bath at 50 °C for 15 min until color development. Absorbance was measured by a spectrophotometer at 820 nm. The concentration of lipid phosphate was determined using disodium hydrogen orthophosphate anhydrous (Na2HPO4) as standard.

Ceramide assay

Ceramide assay was done according to a modified version of the diacylglycerol kinase (DGK) assay by Preiss et al. [18]. First, 200 µl of lipid samples was dried, and then 20 µl of micelles (made of octyl-b-D-glucoside/dioleoyl phosphatidylglycerol) was added per sample. The tubes were sonicated for 30 min in a water bath sonicator. A reaction mixture was prepared of 50 µl 2X buffer (100 nM imidazole HCl pH 6.6, 100 Mm LiCl, 25 mM MgCl2, 2 mM EGTA), 0.2 µl of 1 M DTT (dithiothreitol), 5 µg of diacylglycerol kinase enzyme (DGK, prepared from *E.coli*), and dilution buffer (10 nM imidazole of pH 6.6 and 1 mM diethylenetriaminepentacetic acid, pH = 7). Per sample, 70 µl of the mixture was added, and then the reaction was initiated by adding 10 µl of the ATP mixture made of 2.5 mM cold ATP (non-radioactive) and 1.3 µCi of the [γ-32P] ATP solution in water. The reaction was allowed to proceed for 30 min then stopped by the addition of 2 ml methanol, 1 ml chloroform, and 0.7 ml water. The tubes were allowed to rest for 10 min, and lipids were extracted by adding 1 ml chloroform and 1 ml water. The lipid phase was transferred to a clean glass tube and dried by speed vacuum. Lipids were resuspended in 50 µl of 9:1 ratio chloroform–methanol. Then 25 µl of each sample was spotted on a lane of a silica gel thin-layer chromatography plate. The plates were placed in a previously prepared elution chamber, filled with elution mixture made of chloroform–acetone–methanol–glacial acetic acid–water in a ratio of 50:20:15:10:5. Samples were allowed to migrate for 2 h and then exposed to X-ray film overnight at − 70 °C. The ceramide phosphate bands (identified by comparing them to a known series of ceramide standards) were scrapped into scintillation vials, and 4 ml of scintillation fluid was added. The radioactivity was read using a liquid scintillation counter.

Crude mitochondria isolation

Crude mitochondria were isolated according to a modified version of the assay described by Wieckowski et al. [19]. Cells at a density of 80×10^6 were pelleted, maintained at 4 °C and suspended in 2 ml of cold SB buffer pH 7.4 (250 mM sucrose, 20 mM HEPES–KOH, 10 mM KCl, 1.5 mM MgCl2, 1 mM EDTA, 1 mM EGTA, 1 mM DTT, and 1 × protease inhibitor cocktail). Cells were then completely homogenized manually at 4 °C and the homogenate centrifuged at 600 g for 5 min at 4 °C to get rid of debris and unlysed cells. The supernatant was then centrifuged at 7000 g for 10 min to isolate the crude mitochondrial fraction. The crude mitochondrial fraction that contains the mitochondria with some mitochondrial-associated membranes (MAMs) was washed twice with MRB buffer pH 7.4 (250 mM mannitol, 5 mM HEPES–KOH, 0.5 mM EGTA, and 1 × protease inhibitor cocktail) to remove cytoplasmic contaminations and then stored at − 80 °C for protein and lipid assays. To obtain a cytoplasmic fraction devoid of microsomal and lysosomal contaminations, the supernatant was transferred into a polyallomer tube and centrifuged at 100,000 g for 1 h at 4 °C. The pure cytoplasmic fraction was then stored at − 80 °C for protein and lipid assays.

Protein extraction and quantification

Treated and untreated cells were pelleted at a speed of 1500 rpm for 5 min then resuspended in lysis buffer (0.25 M Tris–HCl pH 6.8, 4% SDS, 20% glycerol and 2 mg bromophenol blue). Samples were boiled for 5 min at 95 °C, and then placed on ice for 20 min. Lysates were then centrifuged at 13,800 rpm and supernatants kept at − 20 °C for quantification. The extracted proteins were quantified using Bio-Rad Protein Assay as described by the manufacturer.

The concentrations of proteins in the samples were identified using different concentrations of Bovine Serum Albumin (BSA, Amersco) as standards.

Western blotting

Protein expression levels were analyzed using acrylamide gels. Samples were prepared with a 1:1 volume ratio of proteins to loading buffer [Tris–HCl 0.25 M (pH 6.8), 4% SDS, 20% Glycerol, 2 mg bromophenol blue, and 5% β-mercaptoethanol] and run using TGS 1X running buffer [TGS 10X: 30 g Tris (hydroxymethyl)-aminomethane, 144 g glycine and 10 g SDS]. The migration was performed at 80 V for the stacking gel and 120 V for the resolving gel. Following migration, transfer to a polyvinylidene difluoride (PVDF) membrane was done in transfer buffer [TGS 1X with 20% methanol] for 90 min at 100 V. Then, the membrane was blocked to prevent non-specific binding using 5% fat-free milk prepared in TBS 1X [TBS 10X: 12 g Tris (hydroxymethyl)-aminomethane and 87.8 g NaCl, pH.8] with 0.1% Tween for 2 h. Following blocking, the membrane was incubated at 4 °C overnight with 2 ml of specific primary antibody diluted in 5% milk-TBS 1 × 0.1% Tween as recommended by the supplier. The membrane was then washed for 10 min with TBS 1 × 0.1% Tween for three cycles and incubated at room temperature for one hour with 5 ml of the horseradish peroxidase-conjugated secondary antibodies (Jackson ImmunoResearch, Europe) diluted in 5% milk- TBS 1 × 0.1% Tween as recommended by the supplier and then another washing cycle for 10 min was done. Finally, the bands were developed using ECL western blotting reagent (GE health care, UK). GAPDH (sc-47724) and actin (sc-1616) were used as loading controls. Antibodies against p53 (DO-1, sc-126), Noxa (Calbiochem; 140,129), Bcl-2 (sc-7382), Cytochrome C (ab90529), SDHB subunit (Succinate dehydrogenase iron-sulfur of complex II; ab14714) and Parp (sc-7150) were used in this study. Densitometric quantification of western blots was performed by ImageJ software (NIH, USA).

Statistical analysis

Statistical significance of the data was determined with a Student's *t* test: *Significant ($P < 0.05$) and **Highly significant ($P < 0.01$) with respect to control.

Results

p53-dependent kinetics of Noxa expression and ceramide accumulation in Molt-4 cells upon γ-irradiation

Noxa is induced within hours of p53 stabilization and precedes the accumulation of ceramide [15]. In order to define the p53-dependent temporal relationships of Noxa expression and ceramide accumulation in Molt-4 cells, we utilized a previously described cellular model of Molt-4 leukemia cells that are either vector infected and contain wild-type p53 (Molt-4-LXSN) or express the human papilloma virus E6 protein, which degrades p53, and thus are functionally p53-null (Molt-4-E6). γ-irradiation (5 Gy) of these cells results in p53 stabilization, followed by ceramide accumulation and apoptosis only in the Molt-4-LXSN cells, whereas the Molt-4-E6 cells are resistant to irradiation [4, 20]. Similar to these published studies, we show here that ceramide levels increased starting at 8 h and reached fivefold of time-matched non-irradiated cells at 24 h in Molt-4-LXSN cells expressing wild-type p53 (Fig. 1a). As expected, no ceramide accumulation was observed in p53-deficient Molt-4-E6 cells (Fig. 1a). Next, we examined the temporal expressions of two p53-inducible genes of the BH3-only subfamily of Bcl-2 proteins, *Noxa* and *Puma* by quantitative real-time PCR following irradiation of Molt-4-LXSN cells. Upon irradiation, *Noxa* mRNA levels increased in a biphasic manner and were significantly higher than time-matched non-irradiated control at 2, 4, 8, and 24 h, while no significant differences were observed for *Puma* mRNA levels (Fig. 1b). In order to verify that the Noxa protein levels were also increasing, we examined Noxa protein expression in Molt-4-LXSN and Molt-4-E6 cells by western blot following irradiation (Fig. 1c). Results showed that Noxa protein levels increased by 2 h and were sustained until 6 h post-irradiation. Molt-4-E6 cells that lack functional p53 showed constant Noxa expression during the same time course following irradiation. These studies confirmed the temporal relationships of p53, Noxa, and ceramide where, only in the presence of p53 stabilization, Noxa is expressed within 2 h and ceramide starts to accumulate by 8 h. They also supported our hypothesis that Noxa may be a candidate in regulating p53-dependent ceramide accumulation.

Impact of Noxa knockdown on the response of Molt-4 cells to irradiation

To study the role of Noxa in the p53-dependent ceramide accumulation observed in response to irradiation,

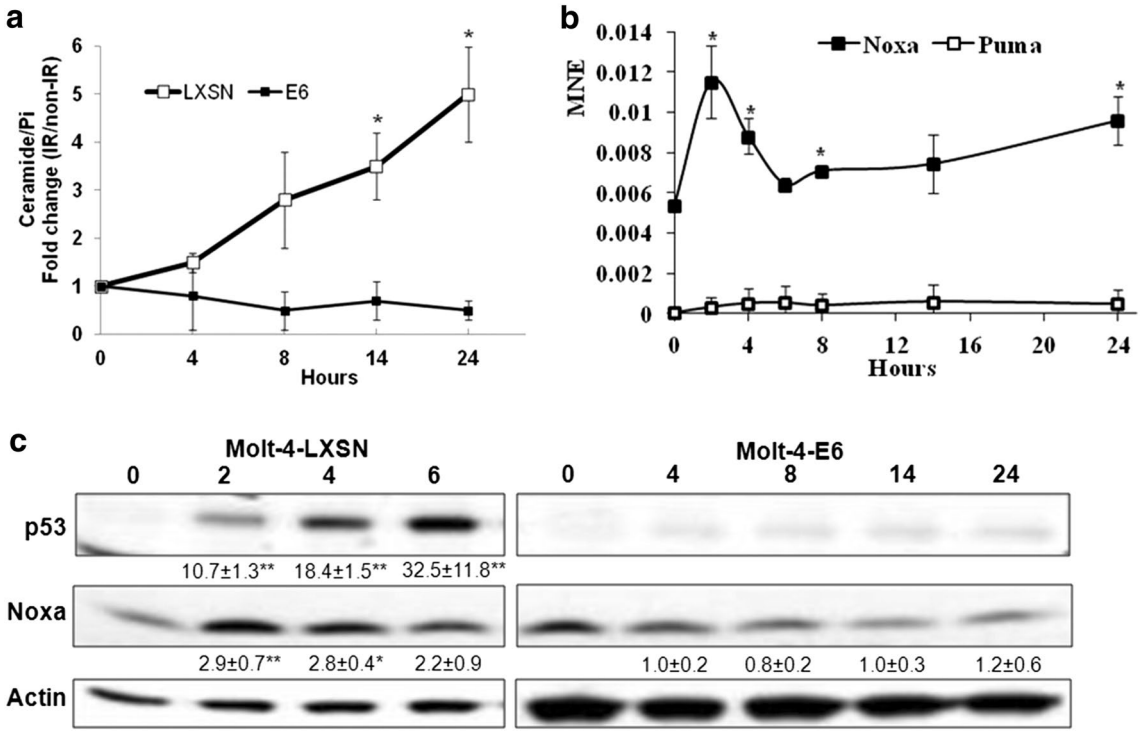

Fig. 1 Ceramide accumulation and p53, Noxa, and Puma expression levels in response to irradiation of Molt-4 cells. **a** The endogenous ceramide accumulation was measured by *E. coli* diacylglycerol kinase assay in Molt-4-LXSN (wild-type p53) and p53-deficient Molt-4-E6 cells at different time points post-irradiation. Ceramide levels in cell lipid extracts were normalized to lipid phosphate. Data are represented as fold change of irradiated (IR) over non-irradiated (IR) time-matched control. Values are represented as mean ± SD of two independent experiments. *Significant difference ($P < 0.05$) with respect to the non-irradiated controls (time point 0). **b** Mean normalized expression (MNE) of *Puma* and *Noxa* in Molt-4-LXSN cells post-irradiation. The mRNA expression level was obtained by quantitative PCR and normalized to *GAPDH* expression. Values are represented as mean ± SD of two independent experiments. *Significant difference ($P < 0.05$) with respect to the non-irradiated controls (time point 0). **c** Protein expression levels of p53 and Noxa in Molt-4-LXSN and Molt-4-E6 cells post-irradiation were assessed on total cell lysates by western blot at different time points (hours). Actin was used as a loading control. Quantification of band intensity was performed by Image J. Values represent the relative expression fold change with respect to non-irradiated controls and are expressed as mean ± SD of three independent experiments. *Significant ($P < 0.05$) and **Highly significant differences ($P < 0.01$) with respect to the non-irradiated controls. Each blot is representative of three independent experiments

we established Molt-4 cells with reduced *Noxa* expression levels. We utilized inhibitory RNA technology using short hairpin RNA (shRNA) that can be stably expressed in transfected cells as described in Methods. We stably transfected Molt-4 cells with either a vector containing a scrambled shRNA sequence or with a vector containing an inhibitory *Noxa (PMAIP1)* shRNA sequence and designated the resulting stable transfectants as SCR and KD^{NOXA}, respectively. Cells were propagated in the presence of hygromycin at a final concentration of 0.5 mg/ml in order to maintain selection pressure. The model was then validated by western blot and showed more than 50% knockdown efficiency of baseline expression of Noxa in KD^{NOXA} cells as compared to SCR cells (Fig. 2a). The response of stable transfectants to irradiation was then assessed for cell death by the trypan blue exclusion assay. Results showed that knockdown of Noxa in Molt-4 cells didn't affect the p53-dependent cell death response as both SCR and KD^{NOXA} cells had almost identical death responses at 10 and 24 h post-irradiation (Fig. 2b). This was confirmed using the apoptosis-specific Annexin V/propidium iodide analysis by flow cytometry. Annexin positive cells significantly increased in comparable intensities in both irradiated models of SCR and KD^{NOXA} cells as compared to their non-irradiated controls after 24 and 48 h post-irradiation (Fig. 2c). We next evaluated the effects of irradiation on PARP cleavage, another indicator of apoptosis, in these cells. Partial PARP cleavage was observed as early as 4 h post-irradiation in both models, SCR and KD^{NOXA}, and complete cleavage was demonstrable at 8 h post-irradiation (Fig. 2d).

The inducible expression levels of Noxa and p53 in irradiated Molt-4-SCR cells confirmed the results obtained for Molt-4-LXSN cells and further validated our Noxa knockdown model (Fig. 3a). The expression level of p53 increased by 2 h and was sustained until 24 h and that of

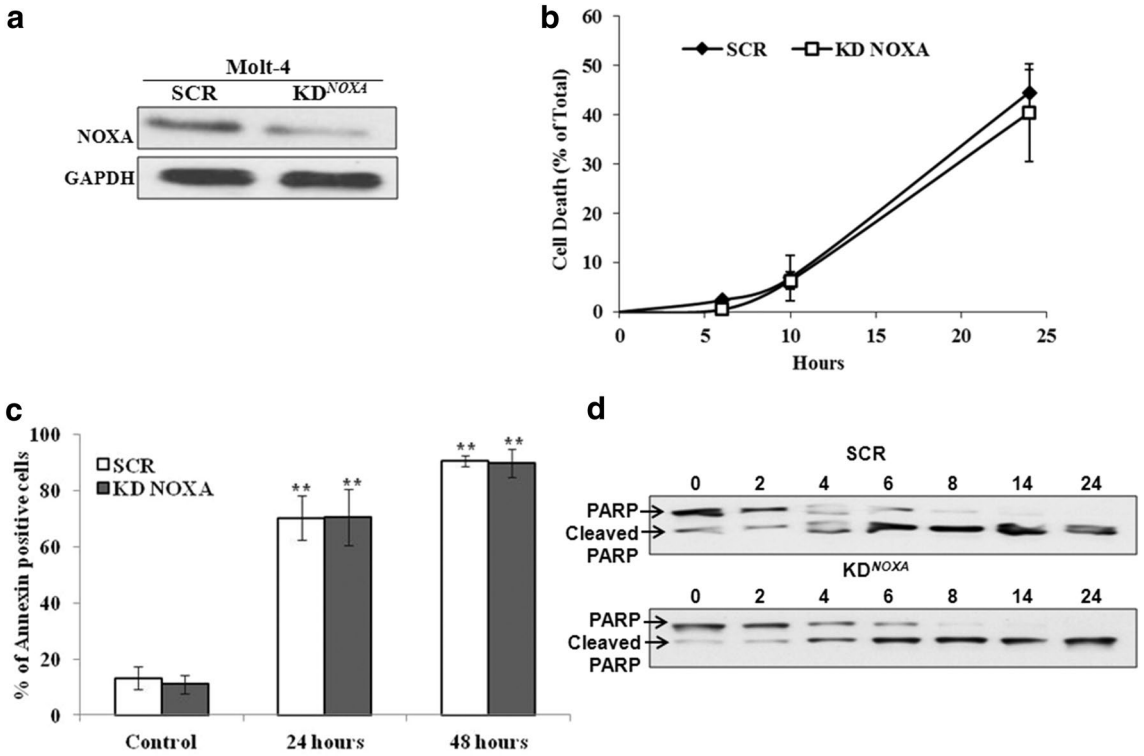

Fig. 2 Establishment and validation of Molt-4 cellular model with reduced levels of Noxa in response to irradiation. **a** Protein expression level of Noxa in Molt-4 cells stably transfected with shRNA scrambled and shRNA *Noxa (or PMAIP1)* designated SCR and KD^{NOXA}, respectively. Total cell lysates were assessed by western blot and GAPDH was used as a loading control. **b** Dead cell count of SCR and KD^{NOXA} in response irradiation. Trypan blue assay was performed on irradiated Molt-4 cells at different time points. Values are presented as percentages of the total cell count and represent the mean ± SD of three independent experiments. **c** Induction of apoptosis in Molt-4 cells in response to irradiation. AnnexinV-FITC/PI flow cytometry analysis was performed on irradiated SCR and KD^{NOXA} cells after 24 and 48 h. Values represent the sum of "Annexin V positive and PI negative" (A + P-) cells and "Annexin V positive and PI positive" (A + P+) cells. Bars are mean ± SD of three independent experiments. **Highly significant difference ($P < 0.01$) of SCR and KD^{NOXA} with respect to their non-irradiated controls. No significance difference between SCR and KD^{NOXA} at the matched time points. **d** PARP cleavage in Molt-4 SCR and KD^{NOXA} was assessed on total cell lysates by western blot at different time points (hours). Each blot is representative of three independent experiments

Noxa increased by 2 h and lasted until 6 h after which it decreased. Moreover, in Molt-4-KD^{NOXA} cells, down regulation of *Noxa* did not affect p53 expression, which confirms that p53 positions upstream of Noxa in our biochemical model. Altogether, these results show that *Noxa* knockdown does not affect the p53-dependent apoptotic response of Molt-4 cells to irradiation indicating that alternative pathways are mediating these effects.

p53-dependent mitochondrial targeting of Noxa and ceramide

Although Noxa was not essential for the p53-induced apoptotic response, it remained possible that Noxa was involved in the regulation of p53-induced ceramide accumulation. In order to examine this possibility, we examined the impact of *Noxa* knockdown on ceramide levels following irradiation. As expected, ceramide levels in SCR cells were significantly increased to 4 and 7 folds at 14 and 24 h, respectively, as compared to time-matched control. However, ceramide levels in KD^{NOXA} cells increased by only 2 and 4 folds at 14 and 24 h, respectively, when compared to their corresponding non-irradiated controls (Fig. 3b). This indicated an important role for Noxa in mediating p53-dependent ceramide accumulation.

Mitochondria are an important hub for apoptotic signaling, including that initiated by p53. Previous studies had demonstrated that Noxa exerts its activity at the mitochondria by interacting with other pro-apoptotic members of the Bcl-2 family of proteins, such as Bak and Bax, and inhibiting the anti-apoptotic ones such as Bcl-2 and Mcl-1 [21]. On the other hand, the accumulation of ceramide at the mitochondrial membrane was demonstrated to be essential for its apoptotic activities [22–24]. Therefore, it became important to assess the translocation of ceramide and Noxa to the mitochondria in this p53-dependent model. We prepared cytosolic and crude

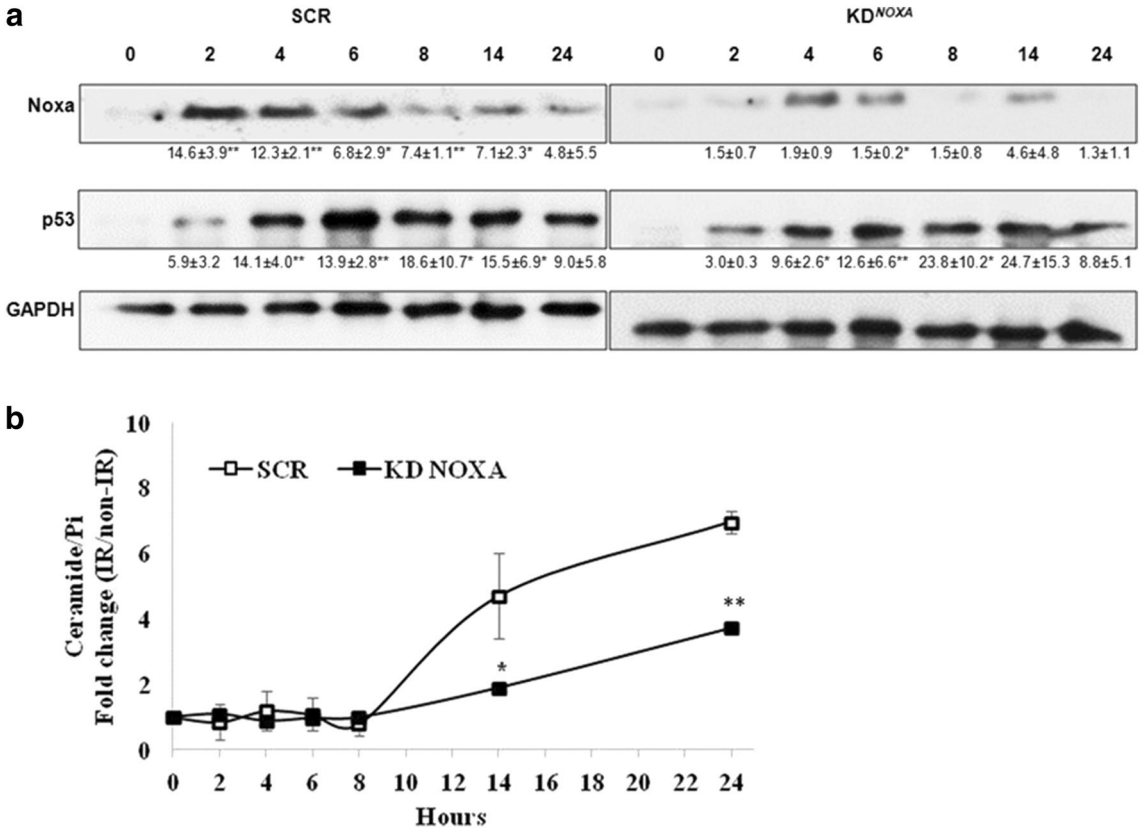

Fig. 3 Impact of Noxa low levels on p53 expression and ceramide accumulation in response to irradiation of Molt-4 cells. **a** Noxa and p53 expression levels in Molt-4 SCR and KD^{NOXA} cells post-irradiation were assessed on total cell lysates by western blot at different time points (hours). GAPDH was used as a loading control. Quantification of band intensity was performed by Image J. Values represent the relative expression fold change with respect to non-irradiated controls and are expressed as mean ± SD of three independent experiments. *Significant ($P < 0.05$) and **Highly significant differences ($P < 0.01$) with respect to the non-irradiated controls. Each blot is representative of three independent experiments. **b** Endogenous ceramide accumulation was measured by *E. coli* diacylglycerol kinase assay in SCR and KD^{NOXA} at different time points post-irradiation. Ceramide levels in cell lipid extracts were normalized to lipid phosphate. Data are represented as fold change of irradiated (IR) over non-irradiated (IR) time-matched control. Values are represented as mean ± SD of three independent experiments. *Significant difference ($P < 0.05$) and **Highly significant difference ($P < 0.01$) with respect SCR

mitochondrial fractions of irradiated SCR cells and measured Noxa, ceramide and cytochrome C levels in both fractions (Fig. 4). Results showed prominent Noxa expression at 2 h post-irradiation in the mitochondrial fraction but this was lacking in the cytosolic fraction (Fig. 4a). Then, we measured ceramide accumulation in both mitochondrial and cytosolic fractions. Mitochondrial ceramide increased significantly at 8 h post-irradiation to reach threefold of baseline at 24 h. In contrast, the increase in cytosolic ceramide was not significant as compared to non-irradiated controls (Fig. 4b). Increases in cytochrome C levels in the cytosol were not appreciable until 8 h post-irradiation.

Relation between Bcl-2, Noxa and ceramide in Molt-4 cells in response to irradiation

Since anti-apoptotic Bcl-2 protein plays a crucial role in inhibiting apoptosis, it was important to understand the biochemical position of Bcl-2 protein relative to p53, Noxa, and ceramide in irradiation-induced apoptosis. In order to investigate the role of Bcl-2 in our model, Molt-4 Bcl-2 cells were established by stably transfecting Molt-4 cells with MEP4 vector expressing *Bcl-2*. The expression level of Bcl-2 was validated and showed an overexpression in Molt-4 Bcl-2 cells as compared to MEP4 control cells (Fig. 5a). Cells

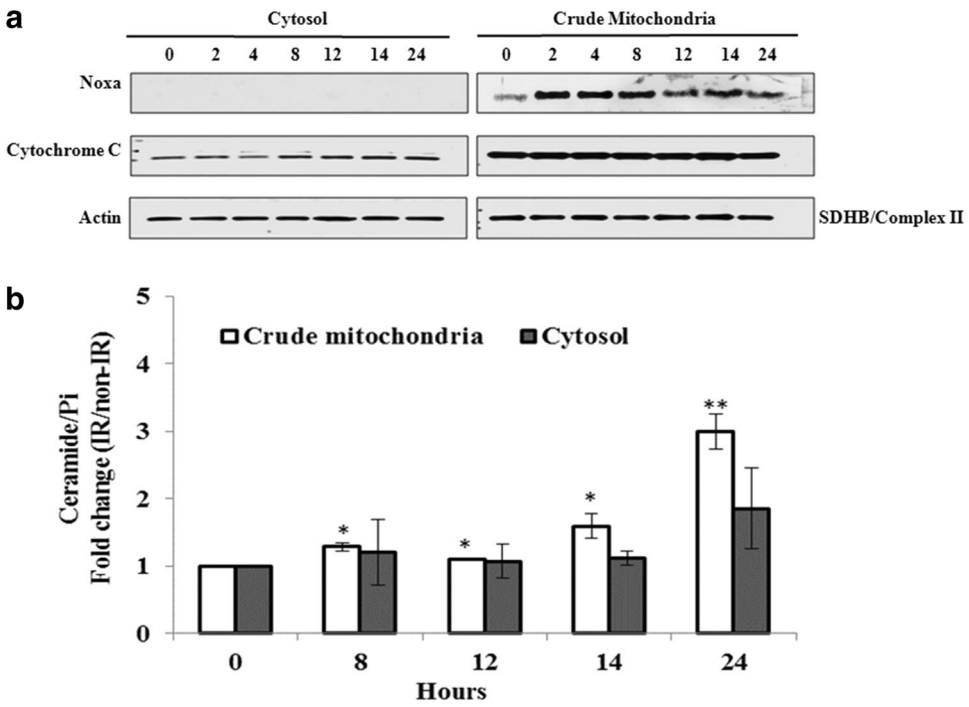

Fig. 4 Noxa, Cytochrome C, and ceramide levels in cytosolic and crude mitochondrial fractions of irradiated Molt-4-SCR cells. **a** Noxa and cytochrome C expression levels in Molt-4-SCR post-irradiation were assessed on cytosolic and crude mitochondrial fractions by western blot at different time points (hours). Actin was used as a loading control for the cytosolic fractions. SDHB subunit of complex II is a marker of the mitochondria and was used as a loading control for the mitochondrial fraction. Each blot is representative of three independent experiments. **b** Endogenous ceramide accumulation was measured by *E. coli* diacylglycerol kinase assay in cytosolic and crude mitochondrial fractions of irradiated Molt-4-SCR at different time points post-irradiation. Ceramide levels in cell lipid extracts were normalized to lipid phosphate. Data are represented as fold change of irradiated (IR) over non-irradiated (IR) time-matched control. Values are represented as mean ± SD of two independent experiments. *Significant ($P < 0.05$) and **Highly significant differences ($P < 0.01$) with respect to their non-irradiated controls. No significance difference between crude mitochondria and cytosol fractions at the matched time points

were then irradiated and collected at different time intervals. First, we examined the effect of Bcl-2 overexpression on p53 and Noxa levels. As shown in Fig. 5b, Bcl-2 overexpression did not affect the expression profiles of p53 and Noxa at 2, 4, and 6 h post-irradiation that were similar to those previously observed in Molt-4 cells. Then, we examined the effect of Bcl-2 expression on cellular ceramide accumulation. As shown in Fig. 5c, Bcl-2 expression completely blocked ceramide accumulation when compared to the control MEP4 cells where ceramide levels increased significantly starting at 8 h and reached 10 folds at 24 h post-irradiation.

Discussion

Studies have shown that γ-irradiation induces p53-dependent apoptosis regulated by Bcl-2 family proteins [25] and that BH3-only pro-apoptotic proteins are central regulators of the p53-mediated apoptosis [26, 27]. We showed in a previous study that the genes of apoptosis signaling pathway (*Bax*, *Bik*, *Jun* and *Bim*), p53 pathway (*Noxa*, *Bax*, *p21*, *TNFRSF10B* and *Fas*), oxidative stress response (*Jun*) and p53 pathway feedback loops 2 (*Mdm2* and *p21*) are differentially expressed in irradiated Molt-4-LXSN cells [15]. These altered candidates localize to the nucleus (*cyclin B1*, *Jun*, *Mdm2* and *p21*), the mitochondria (*Bim*, *Noxa*, *Bax*, and *Bik*), and cell membrane (*Fas* and *TNFRSF10B*) [15]. Stress signaling can regulate the activity of BH3-only pro-apoptotic proteins at different levels such as transcription, mRNA turnover, post-translation and translocation [7]. We have found that upon γ-irradiation, p53 expression increases by 2 h and is sustained until 24 h. Since the promoter region of *Noxa* gene contains a p53 responsive element [25], the tumor suppressor p53 stimulates *Noxa* transcription directly [28]. Indeed, γ-irradiation induces mainly *Noxa* expression and to lower extent *Puma* in Molt-4 leukemia cells (Fig. 1b). The expression level of *Noxa* mRNA increased in a biphasic manner at 2 h and then again at 8 h till 24 h. The first transcriptional phase showed a prominent expression that was illustrated by a significant increase at the protein level (Fig. 1c). The second phase that was observed after 8 h showed a gradual increase and was confirmed at the

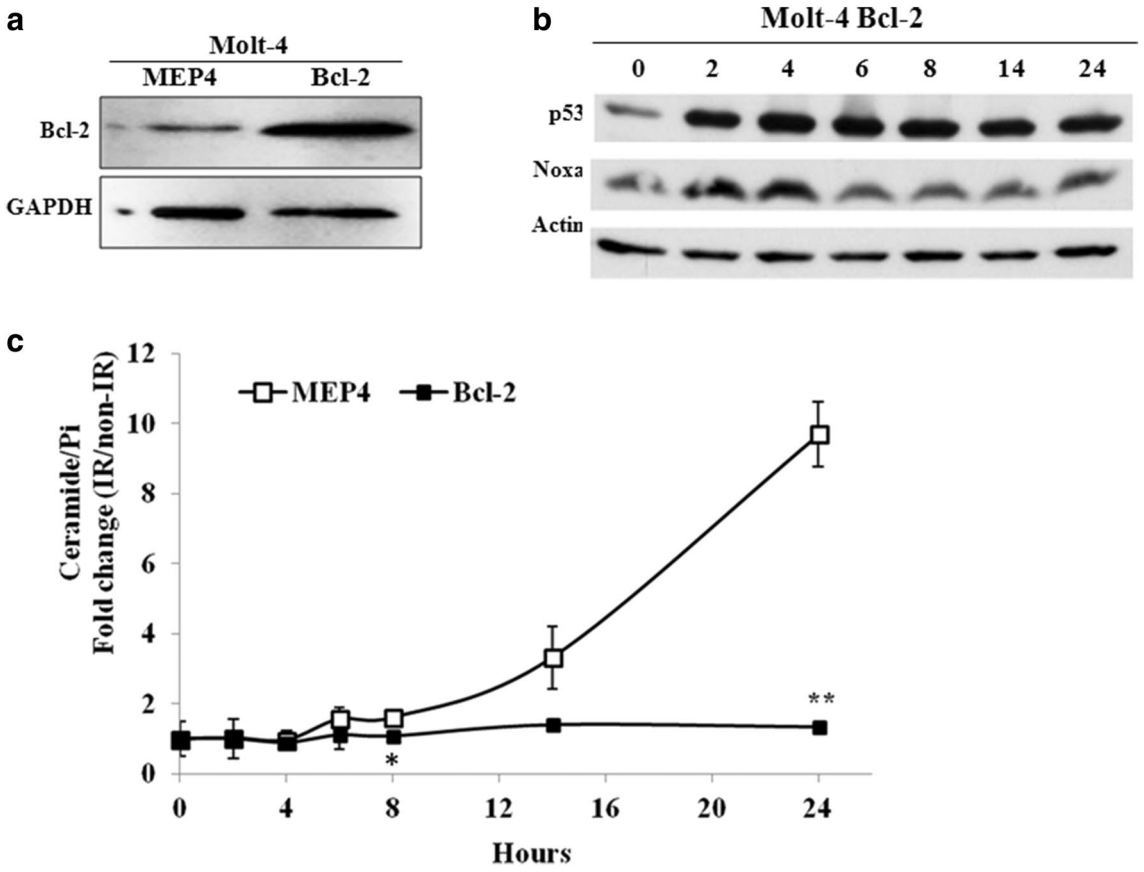

Fig. 5 Establishment and validation of Molt-4 cellular model overexpressing Bcl-2 in response to irradiation. **a** Protein expression level of Bcl-2 in Molt-4 cells stably transfected with MEP4 empty vector and MEP4 vector expressing Bcl-2 designated MEP4 and Bcl-2, respectively. Total cell lysates were assessed by western blot and GAPDH was used as a loading control. **b** Protein expression levels of p53 and Noxa in Molt-4 Bcl-2 cells post-irradiation were assessed on total cell lysates by western blot at different time points (hours). Actin was used as a loading control. Each blot is representative of two independent experiments. **c** Endogenous ceramide accumulation was measured by *E. coli* diacylglycerol kinase assay in MEP4 and Bcl-2 cells at different time points post-irradiation. Ceramide levels in cell lipid extracts were normalized to lipid phosphate. Data are represented as fold change of irradiated (IR) over non-irradiated (IR) time-matched control. Values are represented as mean ± SD of two independent experiments. *Significant ($P < 0.05$) and **highly significant differences ($P < 0.01$) with respect to MEP4 cells

translational level in *Noxa*-expressing SCR cells (Fig. 3a). Moreover, defective p53 was shown to cause a two-fold decrease in *Noxa* expression [29]. Here, we also found that in functionally p53-null Molt-4-E6 cells, Noxa protein levels were downregulated. Upon irradiation of KD^{NOXA} cells, p53 expression levels increased in a similar manner as in *Noxa*-expressing SCR cells, which confirms that p53 acts upstream of Noxa in our model.

Irradiated KD^{NOXA} cells showed similar sensitivity to irradiation as their control Noxa-expressing SCR cells, unlike p53-null cells that showed resistance to irradiation [4]. This validates that in our model Noxa-independent apoptotic pathways are co-activated in response to irradiation [15]. These pathways are not co-dependent in inducing apoptosis, but instead, they are redundant pathways initiated by p53. Our results can be explained by that the intrinsic pathway can still be activated in the absence of Noxa via the activation of other pro-apoptotic proteins and that, possibly, the extrinsic pathway can compensate for the intrinsic apoptosis in the absence of Noxa. Accordingly, abrogation of apoptosis requires simultaneous inhibitions of multiple pathways as demonstrated by Bcl-2, whereas activation of apoptosis in resistant cancer cells may be achieved by activating at least one of them.

Upon irradiation and p53 upregulation, ceramide is generated mainly through de novo ceramide synthesis, specifically associated with ceramide synthase 5, rather than serine palmitoyltransferase, activity in Molt-4 cells [14]. Since the sphingolipid enzymes were not transcriptionally activated in this model [15], it is more likely that de novo ceramide synthesis is regulated by a rapid post-translational activation involving the dimerization of ceramide synthase at the level of the endoplasmic reticulum [30]. In irradiated Molt-4 cells, ceramide could be either generated at the level of the

endoplasmic reticulum by de novo synthesis and then transported to the mitochondria via ceramide transfer protein targeted to the mitochondria (mitoCERT) [31] and mitochondrial-associated membranes (MAMs) or also generated at the level of the mitochondria by mitochondrial ceramide synthases [2].

In our model, Noxa was expressed prior to ceramide accumulation suggesting that it may drive endogenous ceramide synthesis [14]. The level of ceramide in KD^{NOXA} cells was significantly reduced to half upon irradiation suggesting that Noxa is one of the mediators that contribute to ceramide accumulation in our model. One explanation may be that the level of Noxa inhibition we achieved in our system was incomplete and that this "leakiness" may account for the residual accumulation of ceramide observed. An alternative, more likely, explanation is that there are distinct Noxa-independent pathways that also drive ceramide accumulation. We have previously found that *Fas* and *TNFRSF10B* death receptors are upregulated in a p53-dependent manner in irradiated Molt-4-LXSN cells [15]. The Tumor Necrosis Factor (TNF) superfamily is described to initiate endogenous ceramide generation in leukemic cells [32] via sphingomyelinase hydrolysis and de novo synthesis [33]. It is necessary to simultaneously inhibit the two biosynthetic pathways in order to completely abolish ceramide accumulation at both early and late time points and consequently apoptosis in MCF7 and L929 cells [33]. Thus, we can speculate that ceramide accumulation is a common step for both the extrinsic and intrinsic apoptotic pathways in our Molt-4 cellular model.

When the expression level of Noxa was investigated on the crude mitochondrial level, we observed an increase after 2 h that was stabilized till 24 h post-irradiation (Fig. 4a). This suggests that the functional regulation of Noxa is partly through its cellular localization. Thus, Noxa is translocating to the mitochondria immediately post-translation via its mitochondrial targeting domain (MTD) [34], which explains its absence from the cytosolic fraction devoid of mitochondria (Fig. 4a). A recent study revealed that shortly (20 min) after its binding to Bak, Noxa initiates Bak oligomerization and then dissociates from it at longer exposures [35]. Moreover, infected cells with adenovirus-expressing Noxa showed that Noxa completely localized mostly at the mitochondria and partially at the endoplasmic reticulum (ER) triggering both mitochondrial apoptosis and ER stress [25, 36]. Noxa translocation was accompanied by an early and gradual ceramide accumulation in the mitochondrial fractions (Fig. 4b). Ceramide increased significantly starting 8 h in the mitochondria unlike the moderate increase in the cytosolic fraction which suggests that Noxa could be involved in the post-translational activation of ceramide synthase by triggering or facilitating its dimerization at the level of the mitochondria. Based on difference in the total amounts of ceramide between Fig. 3b and 4b, we can suspect that there are other membrane structures associated with ceramide synthesis that could have been eliminated from both the mitochondrial and cytosolic fractions during the experimental procedure.

Mitochondrial ceramide accumulation and cytochrome c release have co-occurred. Increases in cytochrome C levels in the cytosol were not appreciable until 8 h post-irradiation indicating that its release from mitochondria to cytosol, although it occurs following Noxa translocation to the mitochondria, is temporally related to the increase in mitochondrial ceramide. Noxa acts as a facilitator to pave the way for ceramide to contribute to the execution of mitochondrial apoptosis. Thus, ceramide and Noxa may be cooperating in inducing MOMP allowing for cytochrome C release.

The subcellular distribution of Bcl-2 proteins plays an important role in the regulation of apoptosis. Bcl-2 localizes to the ER, the outer mitochondrial membrane and the nuclear membrane as shown by subcellular fractionation [37, 38]. The presence of Bcl-2 at the level of the ER acts as a first line of defense against apoptotic signals and serves to keep pro-apoptotic proteins away from the mitochondria. Moreover, Bcl-2 on the mitochondria inhibits BH3-only proteins that have already accumulated on the mitochondria [39]. The intracellular ratio of Bax/Bcl-2 influences the ability of a cell to respond to an apoptotic signal as well as it predicts the response of certain cancers to some chemotherapeutic agents. Thus, the overexpression of Bcl-2 will tilt the dynamic balance toward anti-apoptotic proteins. Noxa not only binds Mcl-1 and Bcl-xL but also Bcl-2 via BH3 domain. Although Mcl-1 has much higher affinity for Noxa, binding of Noxa to Bcl-2 is potentially important because Bcl-2 is more abundant in certain lymphoid cell lines [40]. The ability of Noxa to disrupt strong Bcl-2/Bim interaction is critically dependent on the ability of Noxa to remain bound to Bcl-2. Upon Bcl-2 expression, the interaction Noxa/Bcl-2 is enhanced and correlates with the protection from bortezomib treatment [40].

To this date, there is no evidence that Bcl-2 directly inhibits its ceramide generation. Bcl-2 overexpression in myeloid HL-60 and lymphoid BL cell lines didn't prevent ceramide generation in response to daunorubicin [41]. Bcl-2 prevented both TNF-α- and ceramide-induced cell death in TNF-α- and Fas-sensitive MCF7 cells but didn't prevent the TNF-α–induced elevation in ceramide levels [42]. These two studies suggested that Bcl-2 functions downstream the ceramide pathway. Other studies showed that Bcl-2 may interfere with ceramide formation. Bcl-2 overexpression in glioma cells blocked neutral sphingomyelinase-mediated ceramide generation and retarded apoptosis by preventing cytochrome c release in response to etoposide, cisplatin and TNF-α [27]. Here, we were able to show that the overexpression of Bcl-2 in irradiated Molt-4 cells completely inhibited the accumulation of ceramide and abrogated cell death (data not shown)

without affecting p53 and Noxa expression levels. Therefore, even if Noxa is not upregulated in response to Bcl-2 overexpression, it could be sequestered by Bcl-2 at the mitochondrial level. One hypothesis could be that the tight binding of Noxa and Bcl-2 leaves more Bcl-xL and Mcl-1 available to tightly bind and inactivate Bax and Bak. Another one is that no free Noxa will be available to interact with and activate Bax and Bak.

Thus, our results suggest that, in our model, Bcl-2 can also act upstream of the de novo ceramide synthesis and can counteract the functions of p53 and Noxa. In addition, we show that a fourfold higher than baseline Bcl-2 protein level is sufficient to inhibit ceramide generation in irradiated Molt-4 cells (Fig. 5a). This means that Bcl-2 expression level can predict the response of certain cancer cells to ceramide-dependent treatments despite their wild-type p53 protein expression levels.

Conclusion

We have shown that silencing Noxa was not enough to inhibit cell death induced by irradiation in Molt-4 cells although ceramide levels were significantly decreased but not completely abrogated. Bcl-2 was found to act not only downstream of ceramide by inhibiting the mitochondrial apoptotic pathway, but also to inhibit the de novo synthesis of ceramide. We provide evidence that ceramide is a critical player in the p53-dependent apoptosis induced by the irradiation of Molt-4 cells and a crosstalk exists between Bcl-2 family members and ceramide to mediate this apoptosis.

Author contributions RHS and GD conceived and designed the project. HK, ZD and LK performed the experiments. HK and RHS analyzed the results. HK and RHS drafted the manuscript. RHS and GD revised and finalized the manuscript which was read and approved by all authors.

Funding This research was supported by funding from the Medical Practice Plan (MPP) at AUB-FM and the Lebanese National Center for Scientific Research (LNCSR) to GD. The funders had no role in study design, data collection and analysis, decision to publish, or preparation of the manuscript.

Compliance with ethical standards

Conflict of interest The authors declare that they have no conflicts of interest with the contents of this article.

References

1. Elmore S (2007) Apoptosis: a review of programmed cell death. Toxicol Pathol 35(4):495–516. https://doi.org/10.1080/01926230701320337
2. Morad SA, Cabot MC (2013) Ceramide-orchestrated signalling in cancer cells. Nat Rev Cancer 13(1):51–65. https://doi.org/10.1038/nrc3398
3. Campaner S, Spreafico F, Burgold T, Doni M, Rosato U, Amati B, Testa G (2011) The methyltransferase Set7/9 (Setd7) is dispensable for the p53-mediated DNA damage response in vivo. Mol Cell 43(4):681–688. https://doi.org/10.1016/j.molcel.2011.08.007
4. Dbaibo GS, Pushkareva MY, Rachid RA, Alter N, Smyth MJ, Obeid LM, Hannun YA (1998) p53-dependent ceramide response to genotoxic stress. J Clin Invest 102(2):329–339. https://doi.org/10.1172/JCI1180
5. Sharpe JC, Arnoult D, Youle RJ (2004) Control of mitochondrial permeability by Bcl-2 family members. Biochim Biophys Acta 1644(2–3):107–113. https://doi.org/10.1016/j.bbamcr.2003.10.016
6. Villunger A, Michalak EM, Coultas L, Mullauer F, Bock G, Ausserlechner MJ, Adams JM, Strasser A (2003) p53- and drug-induced apoptotic responses mediated by BH3-only proteins puma and noxa. Science 302(5647):1036–1038. https://doi.org/10.1126/science.1090072
7. Leber B, Lin J, Andrews DW (2010) Still embedded together binding to membranes regulates Bcl-2 protein interactions. Oncogene 29(38):5221–5230. https://doi.org/10.1038/onc.2010.283
8. Lindsten T, Thompson CB (2006) Cell death in the absence of Bax and Bak. Cell Death Differ 13(8):1272–1276. https://doi.org/10.1038/sj.cdd.4401953
9. Shamas-Din A, Bindner S, Chi X, Leber B, Andrews DW, Fradin C (2015) Distinct lipid effects on tBid and Bim activation of membrane permeabilization by pro-apoptotic Bax. Biochem J 467(3):495–505. https://doi.org/10.1042/BJ20141291
10. Vela L, Gonzalo O, Naval J, Marzo I (2013) Direct interaction of Bax and Bak proteins with Bcl-2 homology domain 3 (BH3)-only proteins in living cells revealed by fluorescence complementation. J Biol Chem 288(7):4935–4946. https://doi.org/10.1074/jbc.M112.422204
11. Colombini M (2017) Ceramide channels and mitochondrial outer membrane permeability. J Bioenerg Biomembr 49(1):57–64. https://doi.org/10.1007/s10863-016-9646-z
12. Bionda C, Portoukalian J, Schmitt D, Rodriguez-Lafrasse C, Ardail D (2004) Subcellular compartmentalization of ceramide metabolism: MAM (mitochondria-associated membrane) and/or mitochondria? Biochem J 382(Pt 2):527–533. https://doi.org/10.1042/BJ20031819
13. Perera MN, Lin SH, Peterson YK, Bielawska A, Szulc ZM, Bittman R, Colombini M (2012) Bax and Bcl-xL exert their regulation on different sites of the ceramide channel. Biochem J 445(1):81–91. https://doi.org/10.1042/BJ20112103
14. Panjarian S, Kozhaya L, Arayssi S, Yehia M, Bielawski J, Bielawska A, Usta J, Hannun YA, Obeid LM, Dbaibo GS (2008) De novo N-palmitoylsphingosine synthesis is the major biochemical mechanism of ceramide accumulation following p53 up-regulation. Prostaglandins Other Lipid Mediat 86(1–4):41–48. https://doi.org/10.1016/j.prostaglandins.2008.02.004
15. Hage-Sleiman R, Bahmad H, Kobeissy H, Dakdouk Z, Kobeissy F, Dbaibo G (2017) Genomic alterations during p53-dependent apoptosis induced by gamma-irradiation of Molt-4 leukemia cells. PLoS ONE 12(12):e0190221. https://doi.org/10.1371/journal.pone.0190221
16. Bligh EG, Dyer WJ (1959) A rapid method of total lipid extraction and purification. Can J Biochem Physiol 37(8):911–917. https://doi.org/10.1139/o59-099
17. Rouser G, Fkeischer S, Yamamoto A (1970) Two dimensional then layer chromatographic separation of polar lipids and determination of phospholipids by phosphorus analysis of spots. Lipids 5(5):494–496

18. Preiss J, Loomis CR, Bishop WR, Stein R, Niedel JE, Bell RM (1986) Quantitative measurement of sn-1,2-diacylglycerols present in platelets, hepatocytes, and ras- and sis-transformed normal rat kidney cells. J Biol Chem 261(19):8597–8600
19. Wieckowski MR, Giorgi C, Lebiedzinska M, Duszynski J, Pinton P (2009) Isolation of mitochondria-associated membranes and mitochondria from animal tissues and cells. Nat Protoc 4(11):1582–1590. https://doi.org/10.1038/nprot.2009.151
20. El-Assaad W, Kozhaya L, Araysi S, Panjarian S, Bitar FF, Baz E, El-Sabban ME, Dbaibo GS (2003) Ceramide and glutathione define two independently regulated pathways of cell death initiated by p53 in Molt-4 leukaemia cells. Biochem J 376(Pt 3):725–732. https://doi.org/10.1042/BJ20030888
21. Morsi RZ, Hage-Sleiman R, Kobeissy H, Dbaibo G (2018) Noxa: Role in Cancer Pathogenesis and Treatment. Curr Cancer Drug Targets 18(10):914–928. https://doi.org/10.2174/1568009618666180308105048
22. Ramirez-Camacho I, Bautista-Perez R, Correa F, Buelna-Chontal M, Roman-Anguiano NG, Medel-Franco M, Medina-Campos ON, Pedraza-Chaverri J, Cano-Martinez A (1862) Zazueta C (2016) Role of sphingomyelinase in mitochondrial ceramide accumulation during reperfusion. Biochim Biophys Acta 10:1955–1963. https://doi.org/10.1016/j.bbadis.2016.07.021
23. Law BA, Liao X, Moore KS, Southard A, Roddy P, Ji R, Szulc Z, Bielawska A, Schulze PC, Cowart LA (2018) Lipotoxic very-long-chain ceramides cause mitochondrial dysfunction, oxidative stress, and cell death in cardiomyocytes. FASEB J 32(3):1403–1416. https://doi.org/10.1096/fj.201700300R
24. Siskind LJ, Kolesnick RN, Colombini M (2002) Ceramide channels increase the permeability of the mitochondrial outer membrane to small proteins. J Biol Chem 277(30):26796–26803. https://doi.org/10.1074/jbc.M200754200
25. Oda E, Ohki R, Murasawa H, Nemoto J, Shibue T, Yamashita T, Tokino T, Taniguchi T, Tanaka N (2000) Noxa, a BH3-only member of the Bcl-2 family and candidate mediator of p53-induced apoptosis. Science 288(5468):1053–1058
26. Hoeferlin LA, Fekry B, Ogretmen B, Krupenko SA, Krupenko NI (2013) Folate stress induces apoptosis via p53-dependent de novo ceramide synthesis and up-regulation of ceramide synthase 6. J Biol Chem 288(18):12880–12890. https://doi.org/10.1074/jbc.M113.461798
27. Sawada M, Nakashima S, Banno Y, Yamakawa H, Takenaka K, Shinoda J, Nishimura Y, Sakai N, Nozawa Y (2000) Influence of Bax or Bcl-2 overexpression on the ceramide-dependent apoptotic pathway in glioma cells. Oncogene 19(31):3508–3520. https://doi.org/10.1038/sj.onc.1203699
28. Ploner C, Kofler R, Villunger A (2008) Noxa: at the tip of the balance between life and death. Oncogene 27(Suppl 1):S84–92. https://doi.org/10.1038/onc.2009.46
29. Huang B, Vassilev LT (2009) Reduced transcriptional activity in the p53 pathway of senescent cells revealed by the MDM2 antagonist nutlin-3. Aging (Albany NY) 1(10):845–854. https://doi.org/10.18632/aging.100091
30. Laviad EL, Kelly S, Merrill AH Jr, Futerman AH (2012) Modulation of ceramide synthase activity via dimerization. J Biol Chem 287(25):21025–21033. https://doi.org/10.1074/jbc.M112.363580
31. Jain A, Beutel O, Ebell K, Korneev S, Holthuis JC (2017) Diverting CERT-mediated ceramide transport to mitochondria triggers Bax-dependent apoptosis. J Cell Sci 130(2):360–371. https://doi.org/10.1242/jcs.194191
32. Bezombes C, Maestre N, Laurent G, Levade T, Bettaieb A, Jaffrezou JP (1998) Restoration of TNF-alpha-induced ceramide generation and apoptosis in resistant human leukemia KG1a cells by the P-glycoprotein blocker PSC833. FASEB J 12(1):101–109
33. Dbaibo GS, El-Assaad W, Krikorian A, Liu B, Diab K, Idriss NZ, El-Sabban M, Driscoll TA, Perry DK, Hannun YA (2001) Ceramide generation by two distinct pathways in tumor necrosis factor alpha-induced cell death. FEBS Lett 503(1):7–12. https://doi.org/10.1016/s0014-5793(01)02625-4
34. Seo YW, Shin JN, Ko KH, Cha JH, Park JY, Lee BR, Yun CW, Kim YM, Seol DW, Kim DW, Yin XM, Kim TH (2003) The molecular mechanism of Noxa-induced mitochondrial dysfunction in p53-mediated cell death. J Biol Chem 278(48):48292–48299. https://doi.org/10.1074/jbc.M308785200
35. Dai H, Smith A, Meng XW, Schneider PA, Pang YP, Kaufmann SH (2011) Transient binding of an activator BH3 domain to the Bak BH3-binding groove initiates Bak oligomerization. J Cell Biol 194(1):39–48. https://doi.org/10.1083/jcb.201102027
36. Kim JY, An YM, Choi WH, Kim JM, Cho S, Yoo BR, Kang JW, Lee YS, Lee YJ, Cho J (2017) Pro-apoptotic Noxa is involved in ablative focal irradiation-induced lung injury. J Cell Mol Med 21(4):711–719. https://doi.org/10.1111/jcmm.13014
37. Krajewski S, Tanaka S, Takayama S, Schibler MJ, Fenton W, Reed JC (1993) Investigation of the subcellular distribution of the bcl-2 oncoprotein: residence in the nuclear envelope, endoplasmic reticulum, and outer mitochondrial membranes. Cancer Res 53(19):4701–4714
38. Janiak F, Leber B, Andrews DW (1994) Assembly of Bcl-2 into microsomal and outer mitochondrial membranes. J Biol Chem 269(13):9842–9849
39. Thomenius MJ, Wang NS, Reineks EZ, Wang Z, Distelhorst CW (2003) Bcl-2 on the endoplasmic reticulum regulates Bax activity by binding to BH3-only proteins. J Biol Chem 278(8):6243–6250. https://doi.org/10.1074/jbc.M208878200
40. Smith AJ, Dai H, Correia C, Takahashi R, Lee SH, Schmitz I, Kaufmann SH (2011) Noxa/Bcl-2 protein interactions contribute to bortezomib resistance in human lymphoid cells. J Biol Chem 286(20):17682–17692. https://doi.org/10.1074/jbc.M110.189092
41. Allouche M, Bettaieb A, Vindis C, Rousse A, Grignon C, Laurent G (1997) Influence of Bcl-2 overexpression on the ceramide pathway in daunorubicin-induced apoptosis of leukemic cells. Oncogene 14(15):1837–1845. https://doi.org/10.1038/sj.onc.1201023
42. Dbaibo GS, Perry DK, Gamard CJ, Platt R, Poirier GG, Obeid LM, Hannun YA (1997) Cytokine response modifier A (CrmA) inhibits ceramide formation in response to tumor necrosis factor (TNF)-alpha: CrmA and Bcl-2 target distinct components in the apoptotic pathway. J Exp Med 185(3):481–490. https://doi.org/10.1084/jem.185.3.481